NUMERICAL ANALYSIS OF PRESSURE AND VOID FRACTION WAVES IN A TRANSIENT TWO-PHASE FLOW USING SLUG-TRACKING MODEL

Jessica Leonel Goncalves, jessicalg@fem.unicamp.br
Ricardo Augusto Mazza, mazza@fem.unicamp.br
Faculty of Mechanical Engineering - State University of Campinas, Rua Mendeleyev 200, 13083-860, Campinas, SP, Brazil

Abstract. *Slug flow is found in many industrial processes with large economic interest and occurs with the largest range of gas and liquid flow rates of all two-phase flow patterns. Despite of its intrinsically transient behavior, most models proposed capture only the average flow parameters. The exceptions are the slug tracking models, which are able to reproduce bubble and slug transient behavior through the pipe. Although slug tracking is a transient model, it has not been used to study the hydraulic transient behavior such as pressure and void fraction waves, despite of their importance for the oil and gas industry. The main objective of this paper is to study the transient characteristics of the slug flow using slug tracking models proposed in literature and explore their abilities to reproduce pressure and void fraction waves. To achieve this objective, some open source slug tracking models are used to simulate the main slug flow parameters when the gas flow rate at the entrance of a horizontal pipe is increased or decreased. Time history and the speed of pressure and void fraction waves were evaluated.*

Keywords*: void fraction wave, pressure wave, transient slug flow, slug tracking model*

1. INTRODUCTION

The main characteristic of two-phase slug flow is the succession of aerated liquid pistons trailed by elongated gas bubbles, hereafter denominated as cells. The interest in this flow regimen has been justified by many industrial applications where this flow pattern occurs. Also, it is challenging to model and characterize the slug flow pattern. Such difficulties can be attributed to the intrinsic unsteady flow behavior, with liquid slugs and bubbles changing their characteristics in time and space. The intrinsic unsteady behavior is due to the interactions between neighboring cells, which change the cells' frequencies and lengths, hold-up, pressure drop and even making cells disappear as they flow through the line. Therefore, it is possible to say that this flow pattern is not periodic in time and space.

The slug flow studies have begun with Wallis (1969), which used the unit cell concept for the first time to describe the slug liquid followed by an elongated gas bubble. The unit cell has been used by many authors (Dukler and Hubbard, 1975; Fernandes et al., 1983; Taitel and Barnea, 1990) in their mechanistic models. These models were based on a line fulfilled with identical periodic cells and predict the average liquid fractions and pressure drop for given flow rates, but it is impossible to capture the interaction between the cells. With the computational capacity increases in the 90's, new slug flow models capable of capturing the flow parameter distribution as the cell flows through the line have developed and the slug tracking is one of them.

The slug tracking model employs a Lagrangian approach to track the cell boundaries as they evolve downstream the pipe. Many authors have proposed models using such approach, beginning with Taitel and Barnea (1993) who used a kinematic model to predict bubble and slug length through the line. Zheng et al. (1994) developed a model capable of capturing the development and dissipation of liquid slug in hilly terrain. Taitel and Barnea (1998) also presented a new model taking into account the gas compressibility in horizontal flow. A few years later, the model of Taitel and Barnea (1998) was modified to hilly terrain lines (Taitel and Barnea, 2000). Using the Grenier (1997) approach, Franklin (2004) proposed a new model that takes into account the acceleration of the liquid film due the area expansion between the cell tail and liquid slug in the pressure drop. Wang et al. (2006) showed a model with wake effect on the bubble tail and pressure drop due to acceleration. Rodrigues (2009) developed a model that could be used for horizontal, inclined and vertical lines. And more recently, Rosa et al. (2015) proposed a model for horizontal and slightly inclined lines with all previous considerations included plus liquid and gas inertia and their momentum fluxes at cells boundaries.

The main motivation of this paper is to fill the lack of previous studies of transient flow behavior in slug flow. According to Fabre et al. (1995) there are only a few works on this field because of their complexity and lack of theoretical studies, even with vast industrial applicability. This kind of studies have important applications on petroleum industries like production lines startup and shutdown, pigging, artificial lift and secondary oil recovery methods with alternated water and gas injection. There is a transient flow behavior when the operating conditions change, for example, when the inlet liquid or gas flow rate increases or decreases, or in the outlet pressure (Vigneron et al., 1995). Such inlet or outlet changes result in a temporal pressure and void fraction fluctuation, which are identified like pressure and void fraction waves.

The objective of this work is the evaluation of the Taitel and Barnea (1998) and Rosa et al. (2015) slug tracking models' capacity to reproduce pressure and void fraction waves in transient two-phase slug flows. The transient condition is generated when the inlet flow rates is subject to a sudden change. There were two tested conditions, one increasing and

the other decreasing the gas flow rate. In both, the inlet liquid flow rates were maintained constant. The tested cases were chosen because they allow access to the model's capacity to reproduce the wave behavior when there is gas expansion or compression due to the gas phase rate increase or decrease. There was also a comparison made against the analytical pressure wave propagation model proposed by Martin and Padmanabhan (1979).

2. MATHEMATICAL FORMULATION

Figure 1 shows the schematic concept of the unit cell used by slug tracking models. Shown in the figure are the j^{th} cell and their neighbors in duct with diameter D, length L and inclination θ in relation to the horizontal, as well as the nomenclature of the main parameters used in the model development. To obtain the model, mass and momentum conservations laws in the integral form are applied to the j^{th} cell under an inertial and stationary frame reference displayed in Fig. 1. The j^{th} cell interacts with the neighboring cells by exchanging mass and momentum through its front and back positioned as X^j and X^{j-1} from the inlet, respectively. The cell has length L_u and is composed by two regions, the liquid film or elongated bubble and liquid slug with lengths L_f and L_S, respectively. The front of the bubble/liquid film is at position Y^j in relation to the start of the duct with a liquid slug ahead of it. The liquid film may have small gas bubbles, but normally their effects are not taken into account in the slug tracking models. In the film region, all models assumed a non-aerated film and all the gas in this region is in the elongated bubble and transits through the pipe with velocity U_G. Both liquid film and elongated bubble share the same pressure (P_G), which is constant along all the bubble length. The liquid slug may contain small gas bubbles and their effects are considered in the model. The liquid slug's gas bubble has a different velocity (U_b) than the slug's liquid velocity (U_S) and it is calculated using a constitutive relationship. The liquid film (R_f) and liquid slug (R_S) holdup are the liquid volumetric fractions in their areas. The wet perimeter S_S and S_f represent the wall area in contact with the liquid at liquid slug and film, respectively. The wall area in contact with the gas is represented by perimeter S_G, and S_i is the interface perimeter between the elongated bubble and liquid film. The fluid properties like density and viscosity of each phase, gas or liquid, are represented by ρ_L, μ_L, ρ_G^j, μ_G, respectively. The gas phase is considered compressible and its behavior is modeled using the perfect gas law in an isothermal flow. The liquid phase is considered incompressible and its density is much higher than the gas phase.

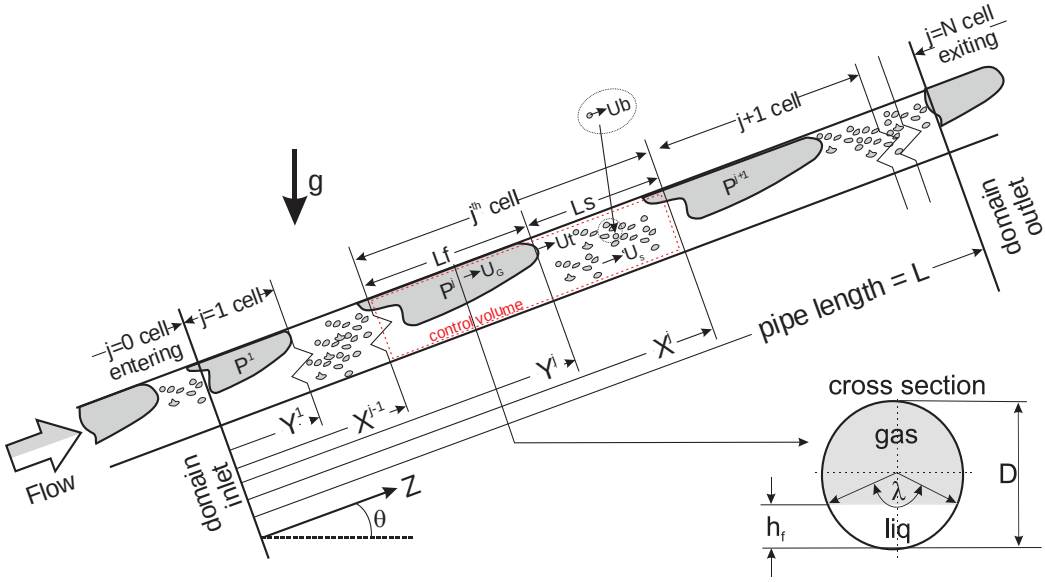

Figure 1. Schematic representation of slug flow with cell properties identifications and positions.

2.1 Closure equation

Slug tracking models are unidimensional and need closure or constitutive equations. For the slug wall shear stress, the homogeneous mixture model is applied by:

$$\tau_S = C_f \frac{1}{2}\rho_M U_M |U_M| \text{ where } C_f = \begin{cases} 0.079/\mathrm{Re}^{0.25} & \text{if } \mathrm{Re}_M > 2{,}000 \\ 16/\mathrm{Re} & \text{if } \mathrm{Re}_M > 2{,}000 \end{cases} \text{ with } \mathrm{Re}_M = \frac{\rho_M U_M}{\mu_M} \quad (1)$$

where C_f is the friction factor, Re_M is the mixture's Reynolds number; ρ_M, μ_M and U_M are the mixture's density, viscosity and velocity, respectively, which are determined using the volumetric liquid fractions in the slug (R_S) by:

$$\rho_M = \rho_L R_S + \rho_G (1-R_S); \quad \mu_M = \mu_L R_S + \mu_G (1-R_S) \text{ and } U_M = U_S R_S + U_b (1-R_S) = J_L + J_G . \tag{2}$$

where J_L and J_G are the superficial gas and liquid velocities, respectively.

The dispersed bubble translational velocity in the liquid slug is calculated with the drift model, $U_b = c_b U_M + u_d$ (apud Taitel and Barnea, 1990), which is written with the liquid velocity in the slug by:

$$U_b = \frac{c_b U_S R_S + u_d}{1 - c_b (1-R_S)} \text{ where } c_b = 1 \text{ and } u_d = 1.54 \left(\frac{\sigma g (\rho_L - \rho_G)}{\rho_L^2} \right)^{1/4} (R_S)^{1.75} \sin\theta . \tag{3}$$

with σ = 0.075N/m being the air-water interfacial surface tension.

The elongated translational bubble velocity (Ut) is calculated by:

$$Ut = \left(C_0 U_M + C_\infty \sqrt{\frac{\Delta\rho}{\rho_L} gD} \right), \tag{4}$$

with C_0 and C_∞ given by Tab. 1.

Table 1 – Default parameters of the bubble translational velocity.

Re_M	Fr_M	C_0	C_∞
≥ 2000	≥ 3.5	1.2	$\frac{0.345}{\left(1+3805/Eo^{3.06}\right)^{0.58}} \mathrm{Sin}\,\theta$
	< 3.5	1.0	$\left(0.542 - \frac{1.76}{Eo^{0.56}}\right) \mathrm{Cos}\,\theta + \frac{0.345}{\left(1+3805/Eo^{3.06}\right)^{0.58}} \mathrm{Sin}\,\theta$
< 2000	-	2.0	$\left(0.542 - \frac{1.76}{Eo^{0.56}}\right) \mathrm{Cos}\,\theta + \frac{0.345}{\left(1+3805/Eo^{3.06}\right)^{0.58}} \mathrm{Sin}\,\theta$

where $Fr_M = U_M / \sqrt{gD}$ and $Eo = (\rho_L - \rho_G) gD^2 / \sigma$.

Considering the interface is represented by a plain surface at the pipe cross section, as shown in Fig. 1, the internal angle θ is related to the liquid film height (h_f) through the trigonometric relation:

$$\lambda = 2\cos^{-1}\left(1 - 2\frac{h_f}{D}\right). \tag{5}$$

The liquid film holdup is defined as a function of the internal angle (θ) by $R_f = (\lambda - \sin\lambda)/2\pi$ and the hydrostatic force acting in the liquid film is determined by the product between the pressure evaluated at the centroid coordinates and the pipe's cross section area taken by the liquid (Mazza et al., 2010). The liquid film centroid coordinate is expressed by:

$$\xi_f = \frac{1}{3\pi R_f} \mathrm{Sin}^3\left(\frac{\lambda}{2}\right) - \frac{1}{2}\mathrm{Cos}\left(\frac{\lambda}{2}\right) \tag{6}$$

2.2 Slug tracking models

Slug tracking models were obtained by the liquid and gas mass balances plus gas-liquid or liquid momentum equation applied to all cell inside the duct. A detailed procedure to obtain the model was shown by Rosa et al. (2015) and the equations shown below represent the mass and momentum equations:

$$K_1 \frac{dP^j}{dt} - K_2 U_S^{j-1} + K_3 U_S^j = K_4 \tag{7}$$

$$K_5 \frac{dU_S^j}{dt} + K_6 U_S^j + P^{j+1} - P^j = K_7 \tag{8}$$

where K_1 to K_7 parameters are coefficients and reflects the hypothesis of each model. For the Rosa et al. (2015) model, the coefficients are shown in Tab. 2. All the coefficients are results from various algebraic manipulations and their physical interpretation are not obvious, however it is possible to establish a connection. The K_1 to K_4 coefficients are related to the conservation of the liquid and gas mass inside the cell where K_1 is the mass gas variation in the film and liquid slug region, K_2 and K_3 are the gas transport in the liquid slug with velocity U_S at the cell's boundaries X^{j-1} and X^j, and K_4 is the liquid slug bubbles' drift velocity. The K_5 to K_7 coefficients are associated with the momentum of the liquid in the cell and their physical interpretation is more complex. The K_5 coefficient represents the rate of change of momentum of the liquid inside the cell. The K_6 coefficient has three parts and the first and second are the rate of efflux of momentum of the liquid crossing the cell boundary and the last is the wall surface tension in the liquid slug. K_7 coefficient has two parts, with the second one associate with the wall surface tension also and the first one with the gravity due to the pipe inclination and to hydrostatic force induced by the liquid film height difference between two consecutives cells.

Table 2. Mass and momentum coefficients in Eqs. (7) and (8).

Parameters	Expressions
K_1	$\left[\left(1-R_f^j\right)L_f^j+\left(1-R_S^j\right)L_S^j\right]/P^j$
K_2	$R_S^{j-1}/\left[1-c_b^{j-1}\left(1-R_S^{j-1}\right)\right]$
K_3	$R_S^j/\left[1-c_b^j\left(1-R_S^j\right)\right]$
K_4	$\frac{\left(1-R_S^{j-1}\right)}{1-c_b^{j-1}\left(1-R_S^{j-1}\right)}u_d^{j-1}-\frac{\left(1-R_S^j\right)}{1-c_b^j\left(1-R_S^j\right)}u_d^j$
K_5	$\rho_L R_S^j L_S^j$
K_6	$\left(R_S^j\rho_L U_S^j\right)\left\{\frac{dL_S^j/dt}{U_S^j}+\left[1-\left(\frac{dx^j/dt}{U_S^j}\right)\right]^2\left(\frac{R_S^j}{R_f^{j+1}}-1\right)+2C_f^j\frac{\rho_m^j}{\rho_L}\frac{\left\|U_M^j\right\|}{U_S^j}\frac{L_S^j}{D}\left[\frac{1}{1-c_b^j\left(1-R_S^j\right)}\right]\right\}$
K_7	$\left(R_S^j\rho_L gD\right)\left[\cos(\theta)\left(\frac{1}{2}-\xi_f^{j+1}\frac{R_f^{j+1}}{R_S^j}\right)-\frac{L_S^j}{D}\sin(\theta)\right]-2C_f\rho_m^j\left\|U_m^j\right\|u_d^j\left(\frac{L_S^j}{D}\right)\left[\frac{\left(1-R_S^j\right)}{1-c_b^j\left(1-R_S^j\right)}\right]$

The temporal pressure (P) and the slug's liquid velocity (U_S) is achieved by applying Eqs. (7) and (8) to all cells inside the pipeline and solving the equations system. The cells' displacement along the duct is calculated by the elongated bubble noise position (Y) and by the translational bubble noise velocity as:

$$Y^{New}=Y^{Old}+Ut.\Delta t\,, \tag{9}$$

where Ut is calculated by Eq. (4) and Δt is the time step adopted in the integration procedure. Furthermore, it is necessary to determine the rate of the liquid slug length, expressed by:

$$\frac{dL_S^j}{dt}\equiv\left(\frac{dx^j}{dt}-\frac{dy^j}{dt}\right)=\frac{\left(1-R_S^j\right)\left(U_b^j-U_b^{j+1}\right)}{\left(R_{f,x^j}-R_S^j\right)}+\left(Ut^{j+1}-Ut^j\right)-\left[\frac{\left(1-R_f^{j+1}\right)L_f^{j+1}+\left(1-R_S^j\right)L_S^{j+1}}{\left(R_{f,x^j}-R_S^j\right)}\right]\left(\frac{1}{P_G^{j+1}}\frac{dP_G^{j+1}}{dt}\right). \tag{10}$$

Rosa et al. (2015) presented a slug tracking model which considers the compressibility effects, satisfies the conservation of liquid and gas mass equation and such momentum of the liquid and the model can be applied to gas and liquid flows in horizontal and slightly inclined ducts. According to the authors, the proposed model is complete because all the unidimensional flow formulation flux terms are considered. The model proposed by Taitel and Barnea (1998) derived by Eqs. (7) and (8) will be described next.

Taitel and Barnea (1998) developed a model considering the gas compressibility and an aerated liquid slug, however the liquid slug volume change due to gas compressibility is not considered. Rosa et al. (2015) assume that the gas density between two consecutives liquid slugs does not change significantly and with these two assumptions it is possible to assure that Eq. (7) also reflects the Taitel and Barnea (1998) model for the mass conservation equation. Taitel and Barnea (1998) considered only the following on their momentum conservation equation: pressure forces, gravity forces due the duct inclination and wall shear stress. Therefore, only the part in K_7 coefficient which reflects the gravity due to the

inclination $\left[\rho_L g R_S^j L_S^j \sin(\theta)\right]$ is maintained and the last part of the K_6 term. The first and second parts in K_6, all remaining K_7 terms and the K_5 coefficient are nulls. Taitel and Barnea (1998) did not considered the momentum efflux at boundaries cells, the hydrostatic force and the rate of change of momentum in the unit cells.

2.3 Numerical model, boundary and initial conditions

The mass and momentum equations represented by Eqs. (7) and (8) together with the closure equations and the time-space displacement of the cell interface, Eqs. (9) and (10), constitute a set of ODEs to be solved in a time and space march process. Eqs. (7) and (8) are discretized using a Crank-Nicholson scheme rendering a tridiagonal system in terms of P and U_S for each cell inside the duct. The entire equation system is solved using an object oriented based algorithm written in FORTRAN. More details about the numerical implementation can be found in Rodrigues (2009).

Before the first cell is introduced inside the duct, it is necessary to setup an initial condition. Usually a monophasic flow with the same flow rate as the mixture flow rate and a constant pressure outlet (P= 99 kPa) is used. The slug tracking can only simulate the slug evolution and all the cell interactions inside the duct, therefore all cell parameters (bubble and liquid slug length, gas and liquid superficial velocities, liquid holdups in the liquid film and slug, and liquid film centroid coordinate) must be informed for all inlet cells. Such parameters must be informed for all cells entering the duct, where the bubble and liquid slug insertion and removal define the simulation conditions. More details about the cell's inlet and outlet can be found in Rosa et al. (2015) or Rodrigues (2009). This work assumes that all entering cells have the same properties and after a specific period of time a sudden inlet parameter change is applied for all new entering cells. A waiting period before the change of the initial steady flow regimen is reached and the simulations goes until the final steady regimen. Two distinct cases are studied in this work, one that increases (Run#1) and other that decreases (Run#2) the gas superficial velocity at the duct inlet as shown in Tab. 3. All inlet cell parameters cited above were obtained from the mean values in experimental campaign of Maria (2016), except for the liquid film centroid coordinate (ξ_f) which was calculated from the liquid film holdup using Eq. (6).

Table 3. Initial and final cell parameters for steady state at inlet for Run #1 and Run#2.

		J_L [m/s]	J_G [m/s]	U_M [m/s]	L_f [m]	L_S [m]	R_f	ξ_f
Run #1	Initial Steady State	0.60	0.54	1.14	0.38	0.17	0.59	0.23
	Final Steady State	0.60	0.27	0.84	0.24	0.15	0.41	0.18
Run #2	Initial Steady State	0.60	0.27	0.84	0.24	0.15	0.41	0.18
	Final Steady State	0.60	0.54	1.14	0.38	0.17	0.58	0.24

3. RESULTS

The numerical procedure is setup at an initial steady state regimen and when a specific cell enters the duct, the new condition is set. Exactly 30 s before the new condition begins, the pressure and the cell void fractions are recorded for every time step at three virtual measuring stations at 4.0 (#1), 10.35 (#2) and 18.64 (#3) m from the inlet. The geometrical and fluid proprieties are: duct diameter and length 0.026 and 22.3 m, respectively; ρ_G = 1,2 kg/m^3, ρ_L = 999 kg/m^3, $\mu_G = 1.7*10^{-5}$ Pa.s, $\mu_L = 8.55*10^{-4}$ Pa.s. For all simulations the time step is 10^{-3} s, in accordance to Rosa et al. (2015)' and Rodrigues (2009)'s mesh test. The slug tracking model can calculate other flow parameters such as L_S, L_f e Ut and the virtual measuring station can capture them for all passing cells. These parameters are out of this paper's scope and will not presented, but it is important to note that the steady regimen finds in this work coincide with previously published finds for both mean values and distributions for these parameters (Franklin, 2004; Rodrigues, 2009; Rosa et al., 2015).

The Fig. 2. (a) and (b) show the cell void fraction and the pressure time history at all virtual stations for Run#1 and #2, respectively using the model of Rosa et al. (2015). In both figures the void fraction has a damping between the two steady state regimens. The final steady regimen for Run#1 is the same as the initial steady regimen for Run#2 for the void fraction, and vice versa. This behavior was expected because Run#1's final steady state was the initial Run#2 steady state. The two slug tracking models tested obtained the same void wave velocity (C_α) as shown in Tab. 4. The first column in Tab. 4 shows between which two stations time was measured to calculate the void fraction and the pressure wave velocity. The next columns are the void fraction and pressure wave velocity obtained with each tested models for both runs. The void fraction wave is 1.08 and 1.35 m/s for Run#1 and #2, respectively. The void fraction wave depends on the bubble nose translational velocity in the final steady regimen, which is 1.08 and 1.37 m/s for Run #1 and #2, respectively. This is because the bubble carries on the biggest portion of the cell gas and is in accordance to Vigneron et al. (1995)

The temporal evolution for the pressure is similar to a shock wave, with a damped jump between the two steady state regimens. The pressure level for the final steady regimen in Run#1 is the same as the initial steady regimen for Run#2, as shown in Fig. 2. For Run#1 the minimal pressure value undershoots the final steady state pressure just after the diminishing of the superficial gas velocity, followed by damped oscillatory pressure recovery to the final steady state.

The pressure for Run#2 has a similar behavior but the maximum pressure value overshoots the pressure on the final steady state. The stations S#1 and S#3 measure the pressure change almost at the same time, but it takes 20 s to establish the final state regimen in the S#3 for Run#1 and 17 s for the Run#2. These time scales are almost the same for the void wave to pass through the entire duct, 17 and 14 s for Run#1 and #2 respectively. The two models presented different pressure waves velocities, as shown in Tab. 4. Taitel and Barnea (1998) calculated a pressure wave velocity of 294.3 m/s for both runs and Rosa et al. (2015) 30.5 and 34.0 m/s for Run#1 and #2 respectively. The Taitel and Barnea (1998) velocity was close to the sound velocity in the air and reflects the absence of the gas compressibility damping factor imposed by the model assumptions. Rosa et al. (2015) shows the influence of the cell liquid acceleration and deceleration ahead of the pressure wave, revealed mainly by the oscillatory pressure behavior shown in Fig. 2. Taitel and Barnea (1998)'s model behavior can be justified by the absence of the terms related to the rate of change of momentum and rate of efflux of momentum across the cell boundaries, making the system stiffer.

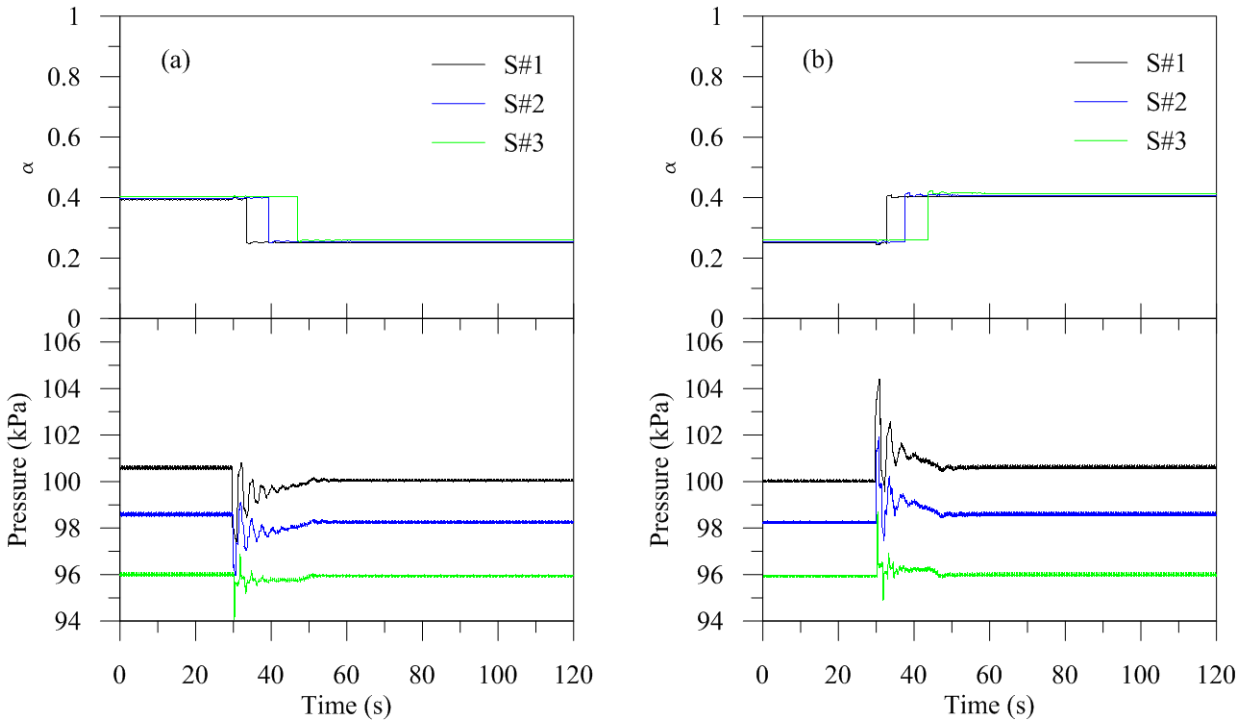

Figure 2 – Temporal evolution of void fraction and pressure at measuring station for Run#1 and Run#2

Table 4. Void fraction and pressure wave velocities obtained by the tested slug tracking models.

Stations	Distance z/D	Run #1				Run #2			
		Taitel & Barnea (1998)		Rosa et al (2015)		Taitel & Barnea (1998)		Rosa et al (2015)	
		C_α (m/s)	C_P (m/s)	C_α (m/s)	C_P (m/s)	C_α (m/s)	C_P (m/s)	C_α (m/s)	C_P (m/s)
S#1 - S#2	280	1.08	317.0	1.08	30.2	1.33	317.0	1.34	31.7
S#1 - S#3	439	1.08	244.0	1.09	30.5	1.34	244.0	1.35	34.1
S#2 - S#3	561	1.08	207.5	1.09	30.7	1.34	207.5	1.35	36.1
Average		1.08	294.3	1.09	30.5	1.34	294.3	1.35	34.0

There are only a few models to establish the pressure wave velocity and the Martin and Padmanabhan (1979) is highlighted because it is a very simple model. The model is based on a homogeneous flow and is:

$$C_P = \sqrt{\frac{kP}{\rho_L \alpha(1-\alpha)}}\,. \tag{11}$$

where P is the absolute pressure, α is the cell's void fraction, ρ_L is the liquid density and k is the atmospheric air isentropic coefficient (k = 1.4). Using the slug tracking results for the pressure and cell's void fraction in the final steady regimen, the pressure waves according with Eq. (11) are calculated and shown in Fig. 3. The figure also shows the pressure wave

calculated by the model of Rosa et al. (2015). Taitel and Barnea (1998)'s results are not presented. The figure shows differences between the two models with a RMS of 4 and 10 for Run#1 and #2 respectively. It is impossible to determine the reason of the difference given that the principles involved in each model are different. Slug tracking model is a dynamic model capable of tracking every single cell throughout the duct allowing the mass and momentum exchange between two consecutive cell and considering each cell stiffs. Martin and Padmanabhan (1979)'s model is based on a sonic wave in a homogenous mixture with no balances applied. Therefore, the slug tracking should show a more realistic result by considering the physics of the phenomenon.

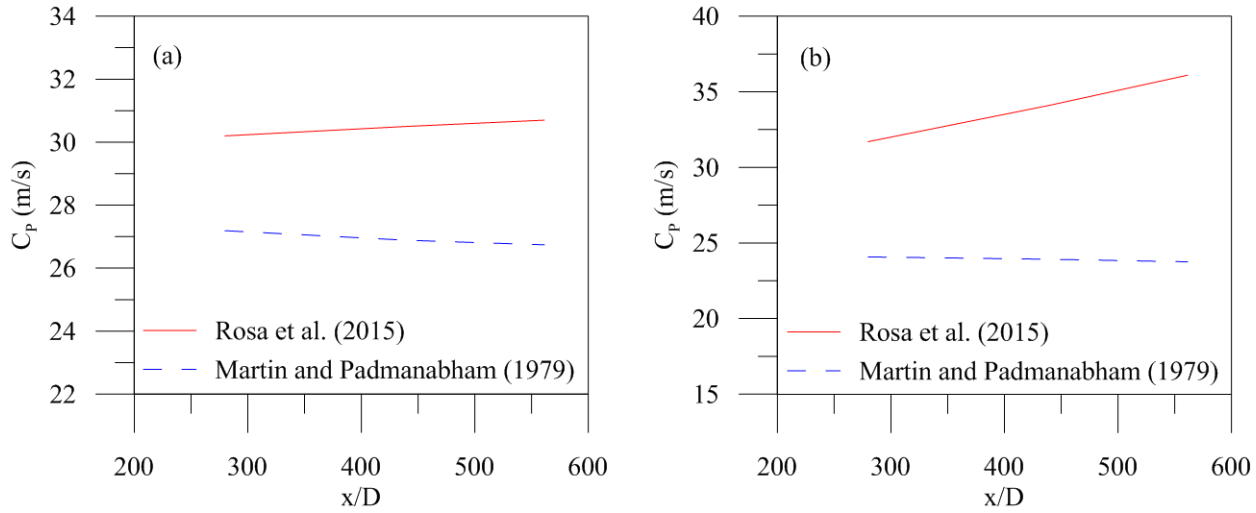

Figure 3. Comparison of pressure wave velocities between slug tracking model (continuous lines) and calculated by Martin and Padmanabhan (1979)'s model (traced line). Run #1 (a) decreasing; Run #2 (b) increasing gas flow rates.

4. CONCLUSION

The transient behavior of a slug flow pattern between two steady state regimens were studied by applying two slug tracking models, Taitel and Barnea (1998) and Rosa et al. (2015). The initial and final steady state regimens at inlet were setup with homogeneous distribution for all cell's parameters. The transient behavior was imposed by a sudden variation, increasing and decreasing the gas flow rate at duct inlet. The pressure and the cell void fraction were measured at three specific distances from inlet to the transient analysis.

The results for the void fraction data was almost the same for both models, but for the pressure it was completely different. Taitel and Barnea (1998)'s model is rigid and there is no oscillation between the two steady state conditions. The pressure wave velocity is of the same order of magnitude of the atmospheric sonic wave. The pressure presents a damped oscillatory motion between the two steady state pressure levels with Rosa et al. (2015)'s model. The pressure damping oscillatory motion is of the same order of magnitude that the time void fraction waves needs to flow through all the duct. The minimum pressure undershot the final steady state pressure level right after the gas flow rate decreased and overshot when the flow rate increased. The typical dynamic terms presented only in Rosa et al. (2015) model such cell's rate of cell momentum change and momentum exchange at cell boundaries are very important to a transient slug flow pattern behavior study.

5. ACKNOWLEDGEMENTS

The authors acknowledge the financial support from CNPq (National Counsel of Technological and Scientific Development).

6. REFERENCES

Dukler, A. E., and Hubbard, M. G., 1975. "A Model for Gas-Liquid Slug Flow in Horizontal and Near Horizontal Tubes." Industrial & Engineering Chemistry Fundamentals, Vol. 14, No. 4, PP. 337–347.

Fabre, J., Liné, A., and Gadoin, E., 1995. "Void and pressure waves in slug flow."In *IUTAM Sypomsium on Waves in Liquid/Gas and Liquid/Vapor Two-Phase Sustems* (pp. 25–44).

Fernandes, R. C., Semiat, R., and Dukler, A. ., 1983. "Hydrodynamic model for fas-liquid slug flow in vertical tubes." AIChE Journal.

Franklin, E. de M., 2004. "*Modelagem Numérica para Seguimento Dinamico de Bolhas em Escoamento Intermitente*

Horizontal Gás-Líquido." Faculdade de Engenharia Mecânica - Universidade Estadual de Campinas.

Grenier, P., 1997. "*Evolution des longueurs de bouchons en écoulement intermittent horizontal*." Institut National Polytechnique.

Maria, L., 2016. "*Estudo Experimental das Ondas de Fração de Vazio e Pressão em Escoamento Horizontal Transiente de Ar e Água no Padrão Intermitente*." Universidade de Campinas.

Martin, C. S., and Padmanabhan, M., 1979. "Pressure Pulse Propagation in Two-Component Slug Flow." Journal of Fluids Engineering, Vol. 101, No. 1, PP. 44.

Mazza, R. A., Rosa, E. S., and Yoshizawa, C. J., 2010. "Analyses of liquid film models applied to horizontal and near horizontal gas-liquid slug flows." Chemical Engineering Science, Vol. 65, No. 12, PP. 3876–3892.

Rodrigues, H. T., 2009. "*Simulação Numérica do Escoamento Bifásico Gás-Líquido no Padrão de Golfadas Utilizando um Modelo Lagrangeano de Seguimento de Pistões*." Universidade Tecnológica Federal do Paraná.

Rosa, Mazza, R. A., Morales, R. E., Rodrigues, H. T., and Cozin, C., 2015. "Analysis of slug tracking model for gas–liquid flows in a pipe." Journal of the Brazilian Society of Mechanical Sciences and Engineering, Vol. 37, No. 6, PP. 1665–1686.

Taitel, Y., and Barnea, D., 1990. "Two-Phase Slug Flow." Advances in Heat Transfer.

Taitel, Y., and Barnea, D., 1993. "A model for slug length distribution in gas-liquid slug flow." International Journal of Multiphase Flow, Vol. 19, No. 5, PP. 829–838.

Taitel, Y., and Barnea, D., 1998. "Effect of gas compressibility on a slug tracking model." Chemical Engineering Science, Vol. 53, No. 11, PP. 2089–2097.

Taitel, Y., and Barnea, D., 2000. "Slug-Tracking Model for Hilly Terrain Pipelines." SPE Journal, Vol. 5, No. 1, PP. 102–109.

Vigneron, F., Sarica, C., and Brill, J. ., 1995. "Experimental analysis of imposed two-phase flow transients in horizontal pipe."In *Proceedings of the BHR Group 7th Internacional Conference* (pp. 199–217). Cannes, França. **i**

Wallis, G. B., 1969. "One Dimensional Two-Phase flow."

Wang, X., Guo, L., and Zhang, X., 2006. "Development of Liquid Slug Length in Gas-Liquid Slug Flow along Horizontal Pipeline: Experiment and Simulation." Chinese Journal of Chemical Engineering, Vol. 14, No. 50536020, PP. 626–633.

Zheng, G., Brill, J. P., and Taitel, Y., 1994. "Slug flow behavior in a hilly terrain pipeline." International Journal of Multiphase Flow, Vol. 20, No. 1, PP. 63–79.

7. RESPONSIBILITY NOTICE

The authors are the only responsible for the information included in this paper.